

Morphology and microstructure of M_2C carbide formed at different cooling rates in AISI M2 high speed steel

X. F. Zhou · F. Fang · F. Li · J. Q. Jiang

Received: 17 December 2009 / Accepted: 3 September 2010 / Published online: 16 September 2010
© Springer Science+Business Media, LLC 2010

Abstract In as-cast structure of AISI M2 high speed steel, M_2C carbide prevails, the morphology of which has crucial influence on distribution and dimension of carbides in final products. In this study, the morphology and microstructure of M_2C formed at different cooling rates have been investigated by scanning electron microscope, X-ray diffraction, transmission electron microscope, and electron back-scatter diffraction. The results show that the morphology of M_2C carbide changes from the plate-like type to the fibrous one with increasing cooling rates. Surprisingly, the microstructure between plate-like and fibrous M_2C is significantly different. Twinning and stacking faults are observed in the plate-like M_2C , which is supported by great misorientations between adjacent carbides. However, no planar faults are identified in fibrous M_2C and the carbides in one colony have almost identical orientation. It is expected that plate-like M_2C grows as a faceted phase, while fibrous M_2C formed at high cooling rates is likely a non-faceted phase. The difference of liquid/solid interface structure is supposed to result in the morphology change of M_2C .

Introduction

High speed steels are widely used in making cutting tools which require high hardness and wear resistance at high temperatures. Among them, AISI M2 steel (Fe–0.9C–6W–5Mo–4Cr–2V, wt%) is the most popular one, owing to good combination of hardness and toughness [1].

The as-cast microstructure of high speed steels consists of matrix and eutectic carbides heterogeneously distributed in interdendritic regions [2]. The main feature of as-cast structure is the morphology and distribution of eutectic carbides, which have crucial influence on mechanical properties of final products [3]. For AISI M2 steel, the predominant type of eutectic carbides is M_2C where M represents a multicomponent group of alloying elements, including W, Mo, V, and Cr. The structure of M_2C can be considered to be a hexagonal close-packed metal sublattice with carbon atoms occupying one half of the octahedral sites [4].

Previous studies have shown that the morphologies of M_2C carbide can be classified as the plate-like type and the fibrous type, depending on the cooling conditions and chemical compositions [5, 6]. Plate-like M_2C is chiefly promoted by low cooling rates or high vanadium, while fibrous M_2C is favored by high cooling rates or additions of minor elements such as nitrogen and calcium [7–9]. However, the mechanism of morphology variation has not been clearly understood yet. Fredriksson has studied the morphology change of M_2C with increasing cooling rates and proposes that it is caused by decreasing segregation of vanadium before eutectic solidification [7]. This hypothesis is contradicted by Boccalini who shows that nitrogen also favors the formation of M_2C in relation to M_6C in which the vanadium content is lower (if the hypothesis is true, the opposite should occur) [5]. He supposes that the change of morphology is related to the supercooling of eutectic reaction.

It is well known that the crystal morphology mainly depends on its structure. In order to clarify the mechanism of morphology change of M_2C , it is necessary to identify the differences of microstructure between the plate-like and the fibrous carbides. Nevertheless, such differences have

X. F. Zhou (✉) · F. Fang · F. Li · J. Q. Jiang
Jiangsu Key Laboratory of Advanced Metallic Materials,
Southeast University, Nanjing 211189, China
e-mail: xfzhou0918@gmail.com

been rarely reported so far. Boccalini et al. [8] and Taran et al. [9] interpret branching of plate-like M_2C by assuming the presence of twinning, but no convincing evidence has been found to support it.

The main objective of this study is to investigate the microstructure and morphological characteristics of M_2C carbide formed at different cooling rates, based on which the possible mechanism of transition is proposed. Different methods including SEM, XRD, TEM, and EBSD have been employed to examine M_2C carbide in detail.

It is important to mention that EBSD is a good complementary method of TEM to investigate the microstructure, which has been widely used to study the microtexture of cubic polycrystals [10, 11]. However, the application to examine carbides with reduced symmetry is relatively rare, e.g., M_2C with HCP structure. In this study, EBSD is used to study the microstructure of M_2C , which supports the results of TEM effectively.

Experimental

Material used in this study was AISI M2 high speed steel, the chemical compositions of which are listed in Table 1. The steel was remelted by a non-oxidation process with a 15 kg medium frequency furnace. Then it was cast in sand and iron cylindrical molds, the dimensions of which were 60 mm × 60 mm × 150 mm and 30 mm × 30 mm × 150 mm, respectively. The specimens were taken from the center at about one-third height of the ingots.

The morphology of carbides was observed by optical microscope using Murakami etchant (3 g $K_3Fe(CN)_6$ + 10 g NaOH + 100 mL H_2O), in which M_2C carbides were etched rather than the matrix [12]. The matrix was deeply etched in an etchant of 5 mL HF + 100 mL H_2O_2 to observe the three-dimensional morphology of carbides by FEI Sirion-400 SEM. The chemical compositions of carbides were also measured using Genesis 60S EDS.

The microstructure of carbides was investigated by different methods, including XRD, EBSD, and TEM.

XRD was carried out in the range of 30–90° glancing angles at a scan speed of 0.2°/min, using XD-3A diffractometer with Cu $K\alpha$ radiation, operating at 40 kV and 30 mA. The specimens for XRD were carbide powders extracted from the corresponding ingots. The extraction of

carbides was performed using electrolysis, operating at 40 V, 0 °C. The electrolyte contained 7 g citric acid, 20 mL hydrochloric acid, and 250 mL methanol.

The samples for EBSD were prepared by a combination of mechanically polishing in diamond suspension and electro-polishing in 5% perchloric acid at 30v, 0 °C for 5 s. The EBSD measurements were carried out by EDAX diffraction system linked to FEI Siron-400 SEM, operating at 20 keV with samples tilted at 70°. The system performed fully automatic indexation of the Kikuchi patterns and automatic calculation of the crystallographic orientation with respect to macroscopic reference axes. The crystal orientation maps were built according to the orientation and color keys. Individual orientation at each qualitatively sampled location was output in numerical format as Euler angles. The misorientations between different points were characterized with Euler angles and calculated automatically by the system.

The specimens for TEM were cut into sections about 800 μ m in thickness and thinned to about 100 μ m by mechanical polishing. Then they were dimpled to disks with 3 mm diameter and 20 μ m thickness using a Gatan precision dimple grinder model 656. An observation hole was finally introduced by a Gatan dual ion milling machine model 600 beam thinner and a Gatan precision ion polishing system model 691. The thin foils were examined by JEM 2000EX TEM, operating at an accelerating voltage of 160 kV.

Further investigation on morphology of carbides in the final products was also carried out. The ingots were prepared as mentioned above. Then, the ingot solidifying in the sand mold was machined to 30 mm × 30 mm × 150 mm, identical to that of the ingot solidifying in the iron mold. They were heated at 1100 °C for 1 h and then forged to square billets with a reduction ratio of 4. Specimens were taken from the center of the billets. The microstructure was examined using SEM.

Results

Morphology of M_2C carbide formed at different cooling rates

Figure 1 shows typical morphologies of eutectic carbides in M2 high speed steel. At low cooling rates, eutectic carbides present a needle-like or plate-like shape, and the interface between eutectic colony and primary grain is ragged (Fig. 1a). At high cooling rates, however, the carbides bend and develop into a fibrous shape (Fig. 1b). Meanwhile, the carbides are refined and the spacing between adjacent carbides also decreases, outlining the interface clearly.

Table 1 Chemical compositions of investigated M2 steel in weight percent

C	Si	Mn	W	Mo	Cr	V	S	P
0.87	0.32	0.26	5.83	4.61	3.99	1.76	0.008	0.027

Balance is Fe

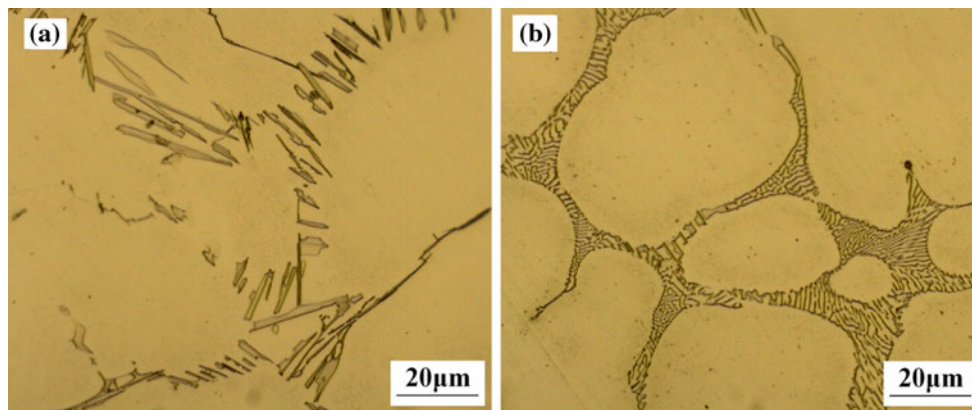


Fig. 1 Typical morphologies of M_2C carbide formed at different cooling rates: **a** plate-like M_2C in the ingot solidifying in sand mold and **b** fibrous M_2C in the ingot solidifying in iron mold

The results of TEM, XRD, and EBSD in this study indicate that both the plate-like and the fibrous carbides are M_2C type. Figure 1 illustrates that the morphology of M_2C carbide changes from the plate-like type to the fibrous one with increasing cooling rates. This is in agreement with previous studies [6, 8].

Detailed observation of the three-dimensional morphology of M_2C reveals that the growing characteristics between the plate-like and the fibrous carbides are totally different (Fig. 2). At low cooling rates, M_2C grows into flat flake, indicating that the growth is anisotropic. The growth rate of orientation perpendicular to the flake is much lower than those of orientations parallel to the flake. Further observation illustrates that the surface of the flake is not smooth (Fig. 3). There are projections on the surface of plates, which are expected to be growth steps at the liquid/solid interface during solidification.

However, as the cooling rates increase, the growth steps disappear. Fewer preferred growth directions are observed. M_2C exhibits a fibrous shape and grows into a dendritic structure with extensive branches, which seem to be the growth characteristics of a non-faceted phase. It suggests that the growing process of M_2C may change

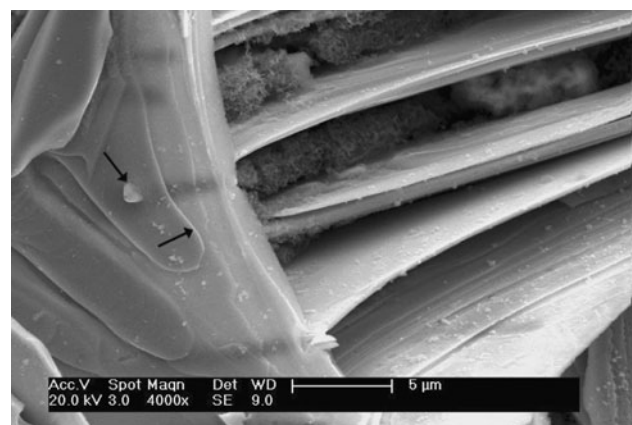


Fig. 3 Morphology of plate-like M_2C examined by SEM. The *arrows* show the projections on the surface of plates, which are expected to be the growth steps

with cooling rates. Further discussion is performed in the later section.

Moreover, it is noted that the amount of alloying elements in M_2C changes greatly with increasing cooling rates (Table 2). Compared with plate-like M_2C , the content of strong carbide forming elements in fibrous M_2C ,

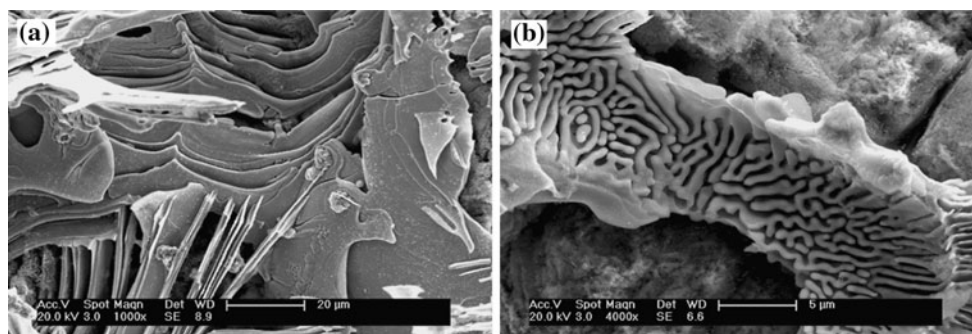


Fig. 2 Three-dimensional morphologies of M_2C carbide after removing the matrix: **a** plate-like M_2C and **b** fibrous M_2C . Two carbides showing different growing characteristics

Table 2 Chemical compositions of M_2C with different morphologies in weight percent

M_2C	Chemical compositions				
	V	Mo	W	Cr	Fe
Lamellar type	12.59	28.05	40.89	6.34	11.50
Rod-like type	5.55	13.35	23.70	5.72	50.68

including vanadium, molybdenum, and tungsten, decreases remarkably.

Microstructure of M_2C carbide formed at different cooling rates

XRD study of M_2C

Figure 4 shows the XRD profiles of carbide powders extracted from the ingots solidifying in the sand and iron mold, respectively. It is found that the carbides in both ingots consist of M_2C and a small amount of MC. The types of carbides in M2 steel are not influenced by cooling rates. However, the relative intensity among diffraction peaks of M_2C changes significantly, particularly for the (0002) peak.

In the XRD profile of fibrous carbide powders, the intensity of (101) peak is the strongest and a little higher than that of (0002) peak (Fig. 4b). The differences of intensity among peaks of M_2C are not remarkable, which is similar to XRD profile of the corresponding ingots. It suggests that fibrous M_2C has fewer special crystallographic planes on the crystal surfaces.

In contrast, the intensity of (0002) peak from the plate-like carbide powders increases greatly compared to that from the ingots (Fig. 4a). Further observation of the plate-like carbide powders using SEM reveals that the original plates are crushed into smaller pieces during the preparation of specimens for XRD. Most of the small plates are nearly parallel to the surface of specimens, which is

expected to cause the increment in intensity of (0002) peak. Thus, it can be inferred that the surface of plates should be parallel to (0002) plane of M_2C .

TEM study of M_2C

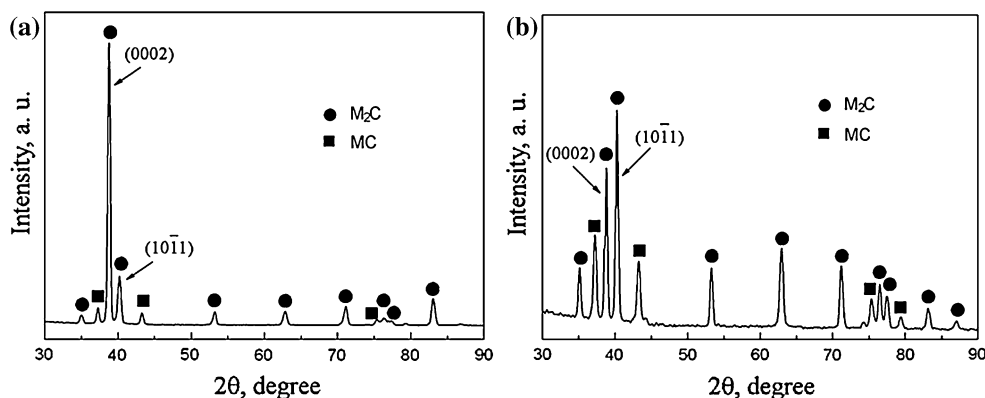
The diffraction patterns from the plate-like and fibrous carbides illustrate that they both have the hexagonal close-packed structure, namely, that they are both the M_2C type, as shown in Fig. 5 [13]. It is also noted that the microstructure differs greatly between the two carbides. In plate-like M_2C , planar faults such as stacking faults and twinning have been observed for the first time. The twinning is parallel to the surface of flake and about 30–50 nm in width (Fig. 5a). These findings strongly support the hypothesis made by Boccacini and Taran, who interpret branching of plate-like M_2C by assuming the presence of twinning [8, 9]. In contrast, few planar faults are identified either in fibrous M_2C or at the branching section of it.

EBSD study of M_2C

Figure 6 illustrates the crystal orientation maps of carbides with different morphologies, which are indexed by the phase of M_2C with hexagonal close-packed structure. The different colors in the maps represent different orientations of the crystal.

It is very interesting to note that the orientations between adjacent plate-like carbides differ greatly, whereas the fibrous carbides in one colony have almost identical orientation. Detailed measurements of Euler angles also demonstrate this point. It shows that the misorientation between branches of plate-like carbides is up to 30–60° while it is within 3° between the fibrous carbides. It is expected that the orientation change in the plate-like M_2C is caused by twinning. Similar results are also obtained from M_7C_3 carbides in high chromium white irons where the carbides in hypo-eutectic alloys present the same

Fig. 4 XRD profiles of carbide powders extracted from: **a** ingot solidifying in the sand mold and **b** ingot solidifying in the iron mold



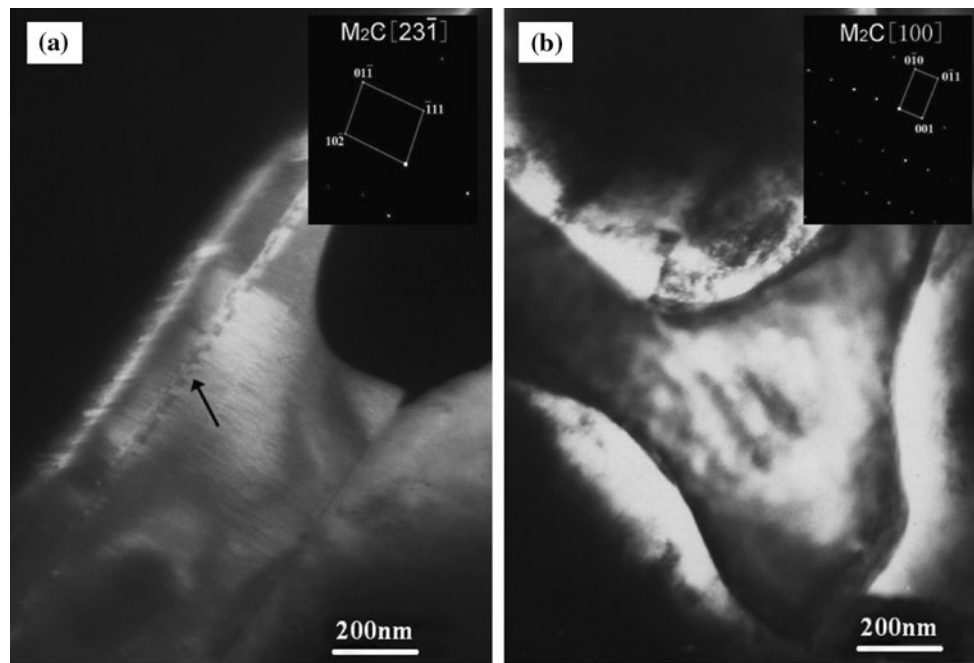


Fig. 5 Microstructure of carbides examined by TEM: **a** dark-field image of plate-like M_2C and **b** bright-field image of fibrous M_2C . The *arrow* in **Fig. 5a** shows the presence of twinning

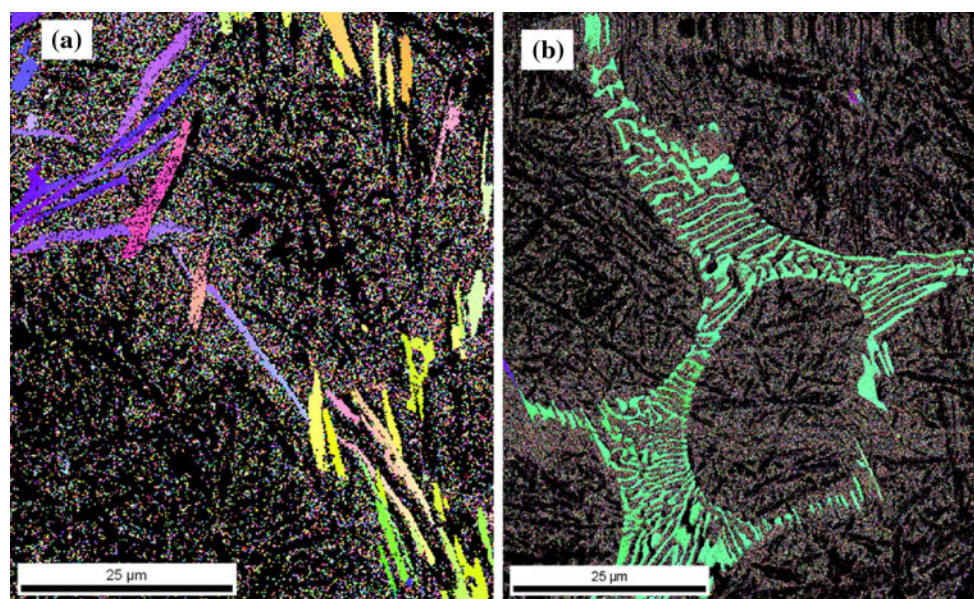


Fig. 6 Orientation maps of the carbides examined by EBSD: **a** plate-like M_2C with different orientations and **b** fibrous M_2C with identical orientation in one colony

orientation while carbides in hyper-eutectic alloys have different orientations [14].

Morphology of carbides in the final products

Figure 7 shows the morphology of carbides in the final products after forging. The primary networks of eutectic carbides in cast ingots have disappeared completely due to

hot deformation. However, the dimensions of the two carbides differ greatly after forging. It is noted that the plate-like carbides remain coarse after forging and the outline is irregular. In contrast, the fibrous carbides are remarkably refined and the average dimensions are almost at the same level as the carbides precipitated from the matrix, which can be attributed to the refined structure and low stability of fibrous M_2C when compared to the case of

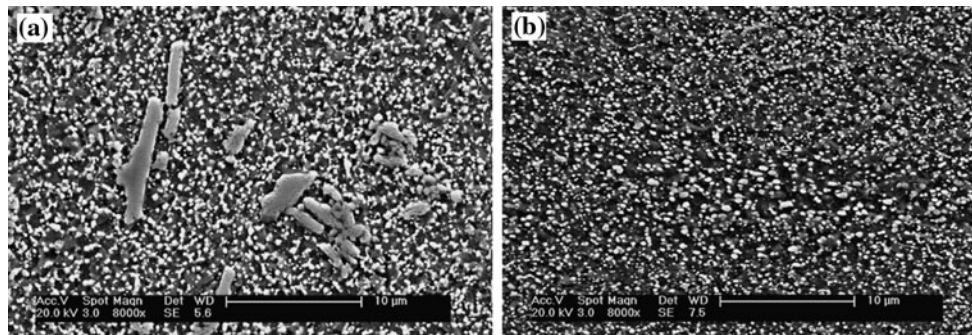


Fig. 7 Microstructure of the billets from: **a** ingot solidifying in sand mold and **b** ingot solidifying in iron mold

plate-like M_2C [15]. It is expected that refined and spherical carbides shown in Fig. 7b can improve the mechanical properties of final products, particularly toughness which is very important for high speed steels [3].

Discussion

Previous results have shown that the morphology of M_2C changes from the plate-like type to the fibrous one with increasing cooling rates. It is known that M_2C carbide is created by the eutectic reaction: liquid \rightarrow austenite + M_2C [2]. During solidification, the crystal morphology is determined by the liquid/solid interface structure which can be classified as the faceted phase and the non-faceted phase [16].

In austenite-carbide eutectics, carbide is generally considered to be a faceted phase owing to its high entropy of melting at low cooling rates [17]. Since the growth of the faceted phase is anisotropic, the crystal planes with higher index grow more rapidly, leaving the close-packed crystallographic planes as the facets on the crystal surfaces. As shown in Fig. 2a, M_2C grows into flat flake, indicating that the growth rate of orientation perpendicular to the flake is much lower than those of other orientations. For M_2C with the hexagonal structure, $\{0001\}$ crystal planes are the most close-packed. Therefore, it is expected that the surface of the flake should be parallel to $\{0001\}$. This is confirmed by the XRD profile of plate-like carbides, which indicates that the surface of plate is parallel to (0002) plane. The lack of (0001) peak is caused by lattice extinction.

Further observation of plate-like M_2C reveals the presence of growth step which is an important characteristic of the faceted phase [17]. During eutectic solidification, liquid atoms deposit on the side of steps and lateral growth of plate-like M_2C occurs. Since the growth of plate-like M_2C is anisotropic, it is difficult to change the growth directions freely. It changes the directions by formation of twinning to prevent the outgrowth of austenite and maintain carbides as

the leading phase [18]. This is confirmed by the TEM and EBSD results of plate-like carbides.

However, it should be noted that the characteristics of the faceted phase disappear at high cooling rates. As shown in Fig. 2b, fibrous M_2C develops into a dendritic structure. Fewer preferred growth directions are observed. The tendency of anisotropic growth becomes less obvious in fibrous carbides. It seems that the growth of fibrous M_2C is more isotropic.

It is known that the liquid/solid interface structure is also influenced by interface undercooling. Given high undercooling, the faceted phase can evolve into a non-faceted phase, which has been confirmed by the change of Si phase in Al–Si alloys [19, 20]. It can be inferred that fibrous M_2C formed at high cooling rates is likely a non-faceted phase, the growth of which is isotropic. The decreasing amount of strong carbide forming elements in fibrous M_2C may also help to reduce the fusion entropy, favoring the transition above. Thus, it could grow freely and change the growth directions without twinning. Identical orientation of fibrous M_2C in one colony also supports this, as shown in Fig. 5b.

Conclusions

To summarize, we have systematically investigated the morphology and microstructure of M_2C formed at different cooling conditions in AISI M2 steel. The results show that the morphology of M_2C changes from the plate-like type to the fibrous one with increasing cooling rates. Although they both have the hexagonal structure, the microstructure of the two carbides is significantly different. Twinning and stacking faults are observed in plate-like M_2C while no planar faults are identified in fibrous M_2C and the carbides in one colony have almost identical orientation. Based upon the morphological characteristics and microstructure, it is expected that plate-like M_2C is a faceted phase whereas fibrous M_2C formed at high undercooling is likely a non-faceted phase.

The difference of liquid/solid interface structure results in the morphology transition of M_2C . Compared with plate-like M_2C , the formation of fibrous M_2C in cast ingots promotes refinement and homogeneous distribution of carbides in the final products, favoring the improvement of mechanical properties.

References

1. Roberts GA, Hamaker JC (1980) Tool steels, 3rd edn. American Society for Metals, Metals Park
2. Fischmeister HF, Riedl R, Karagoz S (1989) Metall Trans A 20A:2133
3. Lee ES, Park WJ, Baik KH et al (1998) Scripta Mater 39:1133
4. Nagakura S, Oketani S (1968) Trans ISIJ 8:265
5. Boccalini M, Goldenstein H (2001) Int Mater Rev 46:92
6. Fredriksson H, Brising S (1976) Scand J Metall 5:268
7. Fredriksson H, Nica M (1979) Scand J Metall 8:243
8. Boccalini M, Matsubara Y, Goldenstein H (1996) AFS Trans 8:907
9. Taran YN, Nizhnikovskaya PF, Snagovskii LM et al (1979) Met Sci Heat Treat 21:791
10. Petrov R, Kestens L, Wasilkowska A et al (2007) Mater Sci Eng A 447:285
11. Hong SH, Lee DN (2003) Mater Sci Eng A 351:133
12. Hetzner DW, Geertruyden WV (2008) Mater Charact 59:825
13. Randle V, Laird G (1993) J Mater Sci 28:4245. doi: [10.1007/BF00351261](https://doi.org/10.1007/BF00351261)
14. Zhou XF, Fang F, Jiang JQ (2008) Foundry 57:658
15. Zhou XF, Fang F, Jiang JQ et al (2009) Kang T'ieh 44:76
16. Flemings MC (1974) Solidification processing, 1st edn. McGraw-Hill, New York
17. Chen Y, Wang HM (2006) J Mater Res 21:375
18. Boccalini M, Correa AVO, Goldenstein H (1999) Mater Sci Technol 15:621
19. Flood SC, Hunt JD (1981) Met Sci 15:287
20. Zhang DL, Cantor B (1993) Metall Trans A 24A:1195